ISPARTA UYGULAMALI BİLİMLER ÜNİVERSİTESİ

Uluslararası Teknolojik Bilimler Dergisi

International Journal of Technological Sciences

UTBD IJTS

Research Article

Performance assessment of PV/T driven transcritical Rankine Cycle: A Comparative study on supercritical working fluids

Gamze Soytürk *[1]

[1]Isparta University of Applied Sciences, Faculty of Technology, Mechanical Engineering, 32200, Isparta, Turkey

Keywords
Photovoltaic/Thermal
Supercritical fluids
Transcritical Rankine Cycle
Energy
Exergy

Article history:
Received: 22.03.2023
Accepted: 25.04.2023

Abstract: The proposed study aims to examine the performance of a combined solar power generation system. The system comprises photovoltaic/thermal (PV/T) panels, a pump, a capacitor, and a turbine. R744, R170, and R41 were used as working fluids. The Engineering Equation Solver (EES) program is used to perform the performance evaluation of the system. Comparative thermodynamic analyzes and parametric studies are conducted to determine the best fluid. The results demonstrate that the highest power production rate of 0.4669 kW is calculated for the cycle using R41, followed by R744. Additionally, the highest energy efficiency and efficiency of exergy are calculated when R41 fluid is used, while the lowest energy and efficiency of exergy are calculated when R170 fluid is used. R170 is determined to have the highest irreversibility, with a destruction rate of exergy of 20.57 kW. According to the results of this analysis, the best working fluid was determined as R41. Parametric analyzes were performed to determine the effects of P_1/P_2 and solar irradiation on the performance of the system, like power production, efficiency of energy, destruction of exergy, and efficiency of exergy. It has been shown that power generation, energy efficiency, and efficiency of exergy increase with P_1/P_2 and solar irradiation for all fluids. While the destruction of exergy decreases with increasing pressure ratio, exergy destruction increases with increasing solar irradiation.

Atıf için/To Cite: Performance Assessment of PV/T Driven Transcritical Rankine Cycle: A Comparative Study on Supercritical Working Fluids. International Journal of Technological Sciences, 15(1), 37-48, 2023.

PV/T destekli transkritik Rankine döngüsünün performans değerlendirmesi: süperkritik çalışma akışkanları üzerine karşılaştırmalı bir çalışma

Anahtar Kelimeler
Fotovoltaik/Termal
Süperkritik akışkanlar
Transkritik Rankine Çevrimi
Enerji
Ekserji

Makale geçmişi:
Geliş Tarihi: 22.03.2023
Kabul Tarihi: 25.04.2023

Öz: Bu çalışmanın amacı, birleşik bir güneş enerjisi üretim sisteminin performansını incelemektir. Sistem, Fotovoltaik/Termal (PV/T) paneller, bir pompa, bir kondansatör ve bir türbinden oluşmaktadır. Çalışma akışkanı olarak R744, R170 ve R41 kullanılmıştır. Sistemin performans değerlendirmesini gerçekleştirmek için Engineering Equation Solver (EES) yazılım programı kullanılmaktadır. En iyi çalışan akışkanı belirlemek için karşılaştırmalı termodinamik analizler ve parametrik çalışmalar yapılır. Sonuçlar, en yüksek güç üretim oranının 0.4669 kW ile R41 ve ardından R744 kullanılan çevrim için hesaplandığını göstermektedir. Ayrıca, en yüksek enerji ve ekserji verimi R41 akışkanı kullanıldığında, en düşük enerji ve ekserji verimi ise R170 akışkanı kullanıldığında hesaplanmıştır. R170'in, 20.57 kW ekserji yok etme oranı ile en yüksek tersinmezliğe sahip olduğu bulunmuştur. Bu analiz sonuçlarına göre en iyi çalışma akışkanı R41 olarak belirlenmiştir. P_1/P_2 ve güneş ışınımının sistem performansı üzerindeki güç üretimi, enerji verimliliği, ekserjinin yok edilmesi ve ekserji verimliliği gibi etkilerini belirlemek için parametrik analizler yapılmıştır. Tüm akışkanlar için P_1/P_2 ve güneş ışınımı ile güç üretim hızı, enerji verimliliği ve ekserji veriminin arttığı gösterilmiştir. Artan basınç oranı ile ekserji yıkımı azalırken, artan güneş ışınımı ile ekserji yıkımı artmaktadır.

*Corresponding author: gamzeyildirim@isparta.edu.tr

1. Introduction

Global energy demand continues to rise due to the significant increase in population and industrial development. Fossil fuels are the most used energy resource on the planet. These traditional energy resources have serious negative environmental consequences, like global warming, greenhouse impact, and pollution of air. To reduce the change of climate and to boost the cycle efficiencies of sustainable and unrenewable technologies, it is crucial to assist the penetration of renewables. Solar energy, which is widely used among renewable energy resources, has gained importance in recent years to meet increasing energy needs. Solar energy is an inexhaustible, clean, environmentally friendly, free energy source that does not emit sulfur, carbon, and gas. Also, due to the consequences of fossil fuels, the development of solar-driven cycles is becoming increasingly important. Improvements to current solar energy-integrated technology are therefore required. Compared to conventional energy sources, these systems provide higher advantages [1].

Solar energy is mainly used for two different purposes: thermal energy and electrical energy. While various technologies are used for these aims, the efficiency of these technologies is rising fast. The conversion of solar energy to thermal energy takes place by solar collectors [2]. Photovoltaic (PV) technologies are widely used to obtain electrical energy directly from solar energy [3]. While PV energy is widely used in small-size applications, PV energy is the most potent option for investigation and improvement for larger-scale use as the manufacture of cheaper PV systems becomes actuality [4]. With PV systems used to obtain electrical energy from solar energy, 15-20% of solar energy can be transformed into electricity, and the remaining energy is converted into thermal energy. This thermal energy can be easily absorbed by the PV device and causes the operating temperature to rise to 80°C [5]. The temperature of the PV solar panel decreases by nearly 0.2-0.5% for each degree Celsius as the solar irradiation increases [6]. This issue can be resolved by using a fluid circulation system that is either naturally occurring or artificially created. PV/T systems, which include combined PV cells and heat sinks, have created an efficient alternative for PV systems by simultaneously supplying electrical and thermal energy [7]. PV/T systems combine thermal collectors and photovoltaic cells to enable the generation of thermal and electrical energy at low temperatures. A schematic representation of a typical PV/T panel is shown in Figure 1. In these systems, the PV cells in contact with the absorber surface convert some of the solar radiation into electrical energy, and the surplus heat energy produced in the PV cells is accepted as the input of the thermal system. During the operation of the system, the heat carrier eliminates this heat from the absorber cells and the surface. Thus, the cells are cooled to obtain thermal energy, and the panel efficiency increases [8]. Different refrigerants, such as air, water, and chemical fluids, can be used in PV/T plants. In addition, according to the physical design of the panels, there are building integrated type, flat plate type, or concentrated PV/T systems [9].

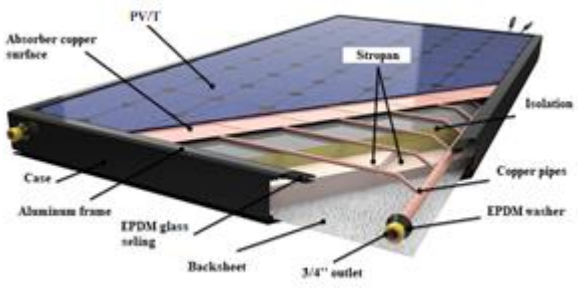

Figure 2. PV/T panel schematic representation [10]

One of the most effective processes for converting thermal energy into power on a big scale is the steam Rankine cycle. H_2O is the best fluid for higher temperature applications and massive centralized systems due to its advantageous features. By choosing a suitable fluid, water-related issues in small and medium-sized power plants can be partially alleviated. In so-named Organic Rankine Cycles (ORC), organic molecules with larger molecular masses and low critical temperatures than water have been suggested [11]. By converting heat into electric energy, ORC, as a lower-grade heat usage technique, can increase energy usage [12]. The ORC can be used in many low-temperature processes, including solar, biomass, geothermal, oceanic, and thermal [13].

Most studies have attempted to improve the system designs and choose the optimum working fluids, such as zeotropic mixes or pure organic fluids, to raise the ORC thermodynamic efficiency [14]. The working fluid has a big impact on how well ORCs perform. Since the application involves a blend of thermal performance, cost, and environmental effects with various heat resource circumstances, it is still difficult to define a global ORC fluid choice criterion. The heat source's energy potential, which also defines the ORC power production system design and the fluid employed, has an important impact on the ORC power production performance of the system [15]. The effects of the single ORC component working fluids' characteristics have also been the subject of numerous investigations. Bahrami et al. [16] proposed three different categories of working fluids with a worldwide warming potential (GWP) of less than 150, including hydrocarbons, hydro fluorochemicals, and mixture working fluids, and evaluated the performance of ORCs in different

configurations based on various performance indicators. Thurairaja et al. [17] investigated how an ORC performed with various working fluids. They used about 100 working fluids that were appropriate for ORCs to carry out the analyses for various temperature ranges. Economic and thermodynamic analyses were carried out for an ORC with PEM electrolyzer by Ganjehsarabi [18]. Analyzes were made using a mixture of pentane, butane, and isopentane as fluid. Yu et al. [19] assessed the effectiveness of an ORC for 22 fluids. The most energy-efficient fluids, according to the data, were R290, R125, R290, and R143a for applications without the use of waste heat and R290, R134a, and R170 for applications that did. To examine how fluid dryness and critical temperature affect the power plant, Song et al. [20] examined a transcritical ORC for 52 various working fluids. This investigation is possibly the most inclusive study carried out for fluids. Xu et al. [21] examined the ORC operating with zeotropic fluids to assess the system's performance advancement. When the studies in the literature were examined, no studies were found on the assessment of the performance of the PV/T-supported ORC cycle for various fluids. Wang et al [22]. presents a zeotropic mixture selection method for ORC with variable heat source temperature. Han et al [23]. proposed the thermodynamic analysis and optimization of an organic Rankine cycle using different zeotropic fluid mixtures as the working fluid, and a flash binary geothermal cycle for both power generation and hydrogen production. In this research, unlike the studies in the literature, it is aimed to examine the performance of the PV/T supported Rankine cycle for R744, R170 and R41 supercritical working fluids. For exergy and energy analysis, a transcritical Rankine cycle is run with the power generated by the PV/T panels. Comparative evaluations of the efficiency of the power cycle are made for various fluids. In addition, parametric studies are carried out to determine the effect of P_1/P_2 and solar radiation on system performance.

2. Choosing Working Fluids

The grade of the ambient temperature, heat resource temperature, the temperature of the coolant liquid, and other factors are taken into consideration while choosing the fluid, which is a crucial step in the ORC process. When developing heat recovery systems, high system efficiency is the major objective, but environmental factors must also be considered for safety and practical reasons. An appropriate fluid for an ORC must meet several specifications. High efficiency, lower global warming potential (GWP), low specific volumes, affordability, moderate pressures, lower toxicity, and lower ozone depletion potential (ODP) are all desirable characteristics. The latter is especially crucial because several high GWP fluids are being phased out as part of ongoing efforts to minimize greenhouse gas emissions. Lastly, safety factors like the maximum permissible concentration and the explosion limit should be considered [24,25]. Additionally, to having zero ODP and low or no GWP, natural refrigerants offer alternatives to several hydrochlorofluorocarbons (HCFC), chlorofluorocarbons (CFC), and hydrofluorocarbon (HFC) type refrigerants [26]. These are substances that are found in nature, like CO2, hydrocarbons, water, ammonia, and air. These materials can serve as cooling agents in air conditioners and refrigerators [27]. The common properties of the fluids are given in Table 1. The critical properties of the fluids given in the table were gained using the EES software. As can be seen from the table, the chosen natural refrigerants have very lower GWP values and zero ODP values. In addition, their atmospheric lifetime is relatively short.

Table 1. Features of supercritical working fluids [1]

Working fluid	ODP	GWP	T_{cr} (°C)	P_{cr} (kPa)
R41	0	92	44.13	5897
R170	0	6	32.17	4872
R744	0	1	30.978	7377

3. System Description

The proposed study aims to examine the performance of a combined solar power generation system. The system comprises photovoltaic/thermal (PV/T) panels, a pump, a capacitor, and a turbine. R744, R170, and R41 were used as working fluids. The system schematic representation is given in Figure 2. The Engineering Equation Solver (EES) program is used to perform the performance evaluation of the system. In the present research, the PV/T system converts solar energy into heat energy and electricity, and the electrical energy produced by the PV/T drives the transcritical Rankine cycle. In this cycle, the fluid is heated by the PV/T up to a supercritical state and sent to the turbine, and the thermal energy is transformed into electrical energy.

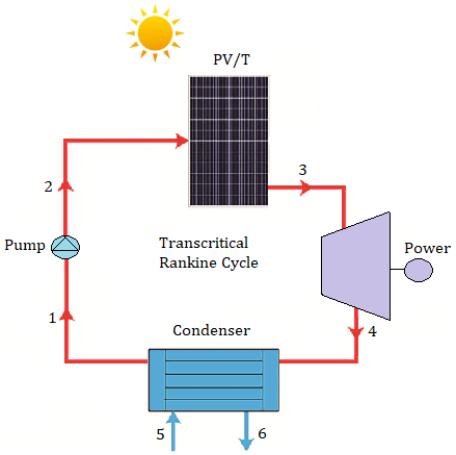

Figure 2. Schematic illustration of PV/T driven transcritical Rankine cycle

The design parameters of the integrated system used in the current research are given in Table 2.

Table 2. Design parameters for the proposed multi-generation system

Parameters	Values
Temperature of reference, T_0 (°C)	19
Pressure of reference, P_0 (kPa)	101.325
Solar irradiation, I_{solar} (W/m²K)	750
Wind speed, V_{wind} (m/s)	2
Pressure ratio, P_1/P_2	1.3
PV/T [28,29]	
Area, $A_{PV/T}$ (m²)	1.63
Cell area, A_{cell} (m²)	1.47
Thickness, L_{si} (m)	$300x10^{-6}$
Thermal conductivity, K_{si} (W/mK)	0.036
Tedlar thickness, L_T (m)	0.0005
Tedlar thermal conductivity, K_T (m)	0.033
Glass thickness, L_g (m)	0.003
Glass thermal conductivity, K_g (m)	1
Absorptivity, α	0.85
Tranmissivity, τ	0.9
Emissivity, ε	0.88
Packing factor, PF	0.9
Reference efficiency, η_{el} (%)	14.3
Temperature coefficient, β (1/K)	0.0045
Number of pipes, n_{pipe}	10
Number of PV/T, $n_{PV/T}$	20
External diameter of pipe, D_{out} (m)	0.008
Internal diameter of pipe, D_{in} (m)	0.006
Insulation thickness, L_i (m)	0.05
Insulation conductivity K_i (m)	0.035
Total mass flow rate, $\dot{m}$ (kg/s)	0.0005
Transcritical Rankine Cycle	
Isentropic efficiency of pump, $\eta_{pump,is}$ (%)	90
Isentropic efficiency of turbine, $\eta_{turbine,is}$ (%)	88

4. Thermodynamic Balance Equations

In this study, the thermodynamic analysis is made under the following assumptions:

- The steady-state and steady-flow conditions are chosen for all system elements.
- The heat losses from the pump, turbine, and compressors are neglected.
- The pressure drops through the pipelines are neglected.
- The turbine and pump operations are assumed to be adiabatic.
- Dead state temperature and pressure are taken as 18°C and 101.325 kPa, respectively.
- The heat transfer between the layers of the PV/T panel is taken into account.

The EES program is used to analyze energy and exergy for the purposes of evaluating the system's performance. The mass and energy balance equations for both steady state and continuous flow systems are expressed as [30]:

$$\sum \dot{m}_{in} = \sum \dot{m}_{out} \tag{1}$$

where, $\dot{m}$ demonstrates the mass flow rate, and subscripts "in" and "out" show the input and output states. Energy balance equality in an overall method is calculated by Equation (2) [31]:

$$\sum \dot{m}_{in}\left(h + \frac{v^2}{2} + gz\right)_{in} + \sum \dot{Q}_{in} + \sum \dot{W}_{in} = \sum \dot{m}_{out}\left(h + \frac{v^2}{2} + gz\right)_{out} + \sum \dot{Q}_{out} + \sum \dot{W}_{out} \tag{2}$$

where, $\dot{Q}$ illustrates the heat energy transfer rate, $\dot{W}$ shows the power transfer rate, h indicates the specific enthalpy, v represents the velocity, z denotes the elevation, and g displays the gravitational acceleration. Entropy balance equality is calculated by Equation (3) as follows:

$$\sum \dot{m}_{in} s_{in} + \sum \frac{\dot{Q}}{T} + \dot{S}_{gen} = \sum \dot{m}_{out} s_{out} \tag{3}$$

In the equation above, s shows the specific entropy, and $\dot{S}_{gen}$ demonstrates the generation rate of entropy. An exergy balance equality of any system could be calculated as [32]:

$$\sum \dot{m}_{in} \dot{ex}_{flow} + \sum \dot{E}x^{Q}_{in} + \sum \dot{E}x^{W}_{in} = \sum \dot{m}_{out} \dot{ex}_{flow} + \sum \dot{E}x^{Q}_{out} + \sum \dot{E}x^{W}_{out} + \dot{E}x_{dest} \tag{4}$$

where $\dot{ex}_{flow}$ represents the exergy of flow, $\dot{E}x^{Q}_{in}$ displays the exergy related to heat flow across the control volume of the process, $\dot{E}x^{W}_{in}$ is the exergy related to work and $\dot{E}x_{dest}$ is the destruction of exergy. In the above equation, each term can be calculated as follows:

$$\dot{e}x_{flow} = (h - h_0) - T_0(s - s_0) \quad (5)$$

$$\dot{E}x^Q = \dot{Q}\left(\frac{T - T_0}{T}\right) \quad (6)$$

$$\dot{E}x^W = \dot{W} \quad (7)$$

$$\dot{E}x_{dest} = T_0\dot{S}_{gen} \quad (8)$$

The capacity of energy, destruction rate of energy, and efficiency of exergy of each system component can be determined by applying the above overall balance equations to individual system components as follows:

Turbine

$$\dot{W}_T = \dot{m}_3(h_3 - h_4) \quad (9)$$

$$\dot{E}x_{dest,T} = \dot{E}x_3 - \dot{E}x_4 - \dot{W}_T \quad (10)$$

Condenser

$$\dot{Q}_C = \dot{m}_6(h_6 - h_5) \quad (11)$$

$$\dot{E}x_{\text{dest,C}} = \dot{E}x_4 + \dot{E}x_5 - \dot{E}x_1 - \dot{E}x_6 \quad (12)$$

Pump

$$\dot{W}_P = \dot{m}_1(h_2 - h_1) \quad (13)$$

$$\dot{E}x_{dest,P} = \dot{E}x_1 - \dot{E}x_2 + \dot{W}_P \quad (14)$$

PV/T panel

The useful heat obtained from the PV/T panel is calculated by Equation (15) [28]:

$$\dot{Q}_u = F_R[I_{solar}(\alpha\tau)(A_{cell} - A_{cell}\eta_{el})] - \left[A_{cell}U_L\left(T_{f,in} - T_{amb}\right)\right] \quad (15)$$

where, $\dot{Q}_u$ (W) is the useful heat provided by the panel, F_R represents the PV/T panel's heat removal factor, I_{solar} (W/m^2) denotes the solar irradiation, $(\alpha\tau)$ shows the absorbance-permeability coefficient, A_{cell} (m^2) is the cell area of PV/T panels, η_{el} indicates electrical efficiency of PV/T panels, U_L (W/m^{2}K) represents demonstrates the overall heat loss coefficient, $T_{f,in}$ (K) shows the fluid inlet temperature and T_{amb} (K) shows ambient temperature. F_R is calculated by Equation (16) as follows [33]:

$$F_R = \frac{\dot{m}c_p}{A_{cell}U_L}\left[1 - exp\left(\frac{-A_{cell}U_L F'}{\dot{m}c_p}\right)\right] \quad (16)$$

Here, $\dot{m}$ (kg/s) denotes the mass flow rate of the heat transfer coefficient, c_p (J/kgK) shows the specific heat capacity, and F' is the panel efficiency factor. The value of F' is a dimensionless number and varies between 0-1 [31]. In this study F' value is accepted as 0.9 U_L (W/m^{2}K), comprises convection, conduction, and irradiation losses from the PV/T panel to the environment, and is calculated by Equation (17) [29]:

$$U_L = U_b + U_{tf} \quad (17)$$

Here, U_b (W/m^{2}K) is the back surface heat loss coefficient from fluid to surroundings (W/m^{2}K), and, U_{tf} (W/m^{2}K) shows the general heat transfer coefficient from glass to air. U_b (W/m^{2}K) could be calculated as follows [29]:

$$U_b = \left[\frac{L_i}{K_i} + \frac{1}{h_{conv}}\right]^{-1} \quad (18)$$

where, L_i (m) denotes insulations thickness on the back surface, and K_i (W/mK) shows thermal conductivity on the back surface. The convection heat transfer coefficient is h_{conv} (W/m^{2}K) expressed as follows [29]:

$$h_{conv} = 2.8 + 3V_{wind} \quad (19)$$

Here, V_{wind} (m/s) shows wind speed. U_{tf} (W/m^{2}K) should be calculated from Equation (6) [29]:

$$U_{tf} = \left[\frac{1}{h_f} + \frac{1}{U_{tT}}\right]^{-1} = \frac{U_{tT}h_f}{U_{tT} + h_f} \quad (20)$$

where, h_f (W/m^{2}K) is the convection heat transfer coefficient of the fluid in the pipe, and U_{tT} (W/m^{2}K) denotes the heat transfer coefficient from glass to Tedlar and is described by Equation (21) [29]:

$$U_{tT} = \left[\frac{1}{U_t} + \frac{1}{U_T}\right]^{-1} = \frac{U_t U_T}{U_T + U_t} \quad (21)$$

Here, U_t (W/m^{2}K) is a general heat transfer coefficient from the solar cell to the environment through glass cover (W/m^{2}K). U_T (W/m^{2}K) represents the conductive heat transfer coefficient from the solar cell to flowing fluid through Tedlar and could be expressed as follows [29]:

$$U_T = \left[\frac{L_{si}}{K_{si}} + \frac{L_T}{K_T}\right]^{-1} \quad (22)$$

where, L_{si}/K_{si} is the conductive resistance term, L_T (m) denotes the thickness of Tedlar, and K_T (W/mK) shows Tedlar thermal conductivity. U_t (W/m^{2}K) could be expressed as given [29]:

$$U_t = \left[\frac{L_g}{K_g} + \frac{1}{h_{conv}} + \frac{1}{h_{rad}}\right]^{-1} \quad (23)$$

Here, L_g (m) denotes glass thickness, K_g (W/mK) shows the thermal conductivity of glass, h_{rad} (W/m^{2}K) is the irradiation heat transfer coefficient and is described as follows [29]:

$$h_{rad} = \varepsilon_g \sigma (T_{sky} + T_{cell})(T_{sky}^2 + T_{cell}^2) \quad (24)$$

where, ε_g displays the emissivity of the glass, σ (W/m^{2}K^4) demonstrates Stefan-Boltzmann's constant, T_{sky} (K) is the sky temperature, and T_{cell} (K) denotes the PV/T panel's cell temperature. T_{sky} (K) is calculated by Equation (25) as follows [28]:

$$T_{sky} = 0.0552 T_{amb}^{1.5} \quad (25)$$

The convection heat transfer coefficient of the fluid in the pipe, h_f (W/m^{2}K), can be calculated as follows [34]:

$$h_f = \frac{Nuk}{D_{in}} \quad (26)$$

Here, k (W/mK) represents the thermal conductivity of the fluid. To determine the heat transfer coefficient of the fluid, the *Reynolds (Re)* number must be calculated first. Re number is calculated by Equation (27) as follows [34]:

$$Re = \frac{4\dot{m}}{\pi D_{in} \mu} \quad (27)$$

where, D_{in} (m) represents the inner diameter of the pipe, and μ_{CO2} (kg/ms) is the dynamic viscosity of the fluid. *Nu* can be expressed as follows [34]:

$$Nu = 0.023 Re^{0.8} Pr^{0.4} \quad (28)$$

Here, Pr denotes the Prandtl number. PV/T surface temperature $T_{PV/T}$ (K) is calculated by Equation (29) [28]:

$$T_{PV/T} = T_{f,in} + \left(\frac{\dot{Q}_u}{A_{cell} F_R U_L}\right)(1 - F_R) \quad (29)$$

The outlet temperature of the fluid from the PV/T panels T_{HTF} (K), is calculated by Equation (30) [28]:

$$T_{f,out} = \frac{\dot{Q}_u}{\dot{m} c_p} + T_{f,in} \quad (30)$$

The electrical power obtained from PV/T is calculated as follows [26]:

$$P_{el} = \eta_{el}\, I_{solar} (\alpha\tau)\, A_{cell}\, n_{pipe} \quad (31)$$

η_{el}, which expresses the electrical efficiency of the panels, should be calculated as given [28]:

$$\eta_{el} = \eta_{el,ref}\left[1 - \beta\left(T_{cell} - T_{amb,ref}\right]\right) \quad (32)$$

where, $\eta_{el,ref}$ represents the electrical efficiency at the reference point, β (1/K) is the temperature power coefficient, and $T_{amb,ref}$ (K) is the reference temperature of the PV/T panel under standard test conditions. The thermal efficiency of PV/T can be determined by Equation (33) [35]:

$$\eta_{th} = \frac{\dot{m} c_p (T_{f,out} - T_{f,in})}{I_{solar}\, A_{cell}} \quad (33)$$

The total efficiency of PV/T panels is calculated by Equation (34):

$$\eta_{top} = \eta_{el} + \eta_{th} \quad (34)$$

The energetic and exergetic efficiency equations for the system could be written as follows:

$$\eta_{en} = \frac{\dot{W}_{net} + P_{el}}{\dot{Q}_{solar}} \quad (35)$$

$$\eta_{ex} = \frac{\dot{W}_{net}}{\dot{E}x_{\dot{Q}_{solar}}} \quad (36)$$

where $\dot{W}_{net}$ is the net power obtained from the system, $\dot{Q}_{solar}$ is solar energy, $\dot{E}x_{\dot{Q}_{solar}}$ is the exergy of the sun and is calculated with the following equations:

$$\dot{W}_{net} = \dot{W}_T - \dot{W}_P \quad (37)$$

$$\dot{Q}_{solar} = n_{PV/T} A_{PV/T} I_{solar} \quad (38)$$

$$\dot{E}x_{\dot{Q}_{solar}} = \dot{Q}_{solar}\left[1 - \frac{4}{3}\frac{T_0}{T_{sun}} + \frac{1}{3}\left[\frac{T_0}{T_{sun}}\right]^4\right] \quad (39)$$

where T_{sun} denotes the temperature of the sun and is 5770°C [36].

5. Results and Discussion

In this research, the thermodynamic performance of the PV/T-supported transcritical Rankine cycle was investigated. At the same time, parametric studies were performed to examine the effects of P_1/P_2 and solar irradiation on cycle performance. In this system, R744, R170, and R41 working fluids are used as heat transfer

fluids. The characteristics of the points for the PV/T-based power cycle seen in Figure 2 are listed in Table 3 for the working fluids. The data shown in the table were determined using the EES software, and the exergy and exergy ratios specific to each point were determined using the equations described in the previous part. As can be seen in the table, some values at points 5 and 6 are negative. This is because of the chosen reference point.

Table 3. Thermophysical properties of each point under specified states

State	Fluid	T (°C)	P (kPa)	ṁ (kg/s)	h (kJ/kg)	s (kJ/kgK)	ex (kJ/kg)	Ėx (kW)
0	R744	19	101.3	-	-6.026	-0.01944	-	
	R170	19	101.3	-	-12.4	-0.03986	-	-
	R41	19	101.3	-	619.5	3.208	-	-
1	R744	20	5729	0.1	-250.9	-1.551	202.6	20.26
	R170	20	3766	0.1	-342.1	-2.07	263.4	26.34
	R41	20	3407	0.1	256.3	1.19	226.3	22.63
2	R744	26.28	9590	0.1	-245.5	-1.549	207.6	20.76
	R170	26.08	6334	0.1	-333.9	-2.067	270.8	27.08
	R41	25.72	7666	0.1	264.1	1.193	233.3	23.33
3	R744	45.59	9590	0.1	-137.1	-1.201	214.2	21.42
	R170	43.85	6334	0.1	-220.9	-1.702	277.2	27.72
	R41	52.35	7666	0.1	371.7	1.536	240.8	24.08
4	R744	20	5729	0.1	-146.9	-1.197	203	20.3
	R170	20	3766	0.1	-232.7	-1.697	263.8	26.38
	R41	20	3407	0.1	359.2	1.542	226.7	22.67
5	R744	15	101.3	0.9933	63.08	0.2244	85.96	85.39
	R170	15	101.3	1.045	63.08	0.2244	92.34	96.51
	R41	15	101.3	0.9837	63.08	0.2244	-539.5	-530.7
6	R744	17.5	101.3	0.9933	73.54	0.2606	85.87	85.29
	R170	17.5	101.3	1.045	73.54	0.2606	92.24	96.41
	R41	17.5	101.3	0.9837	73.54	0.2606	-539.6	-530.8

Figure 3 demonstrates the net power from the PV/T-based cycle for various working fluids. According to the analysis results, the highest net power output of 0.4669 kW was obtained for supercritical fluid R41, succeeded by R744 and R170.

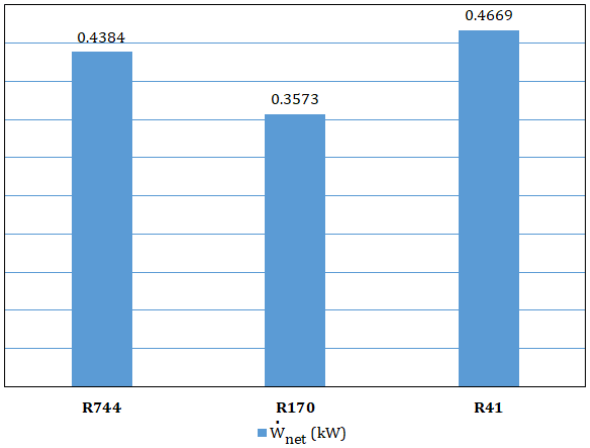

Figure 3. Net power from PV/T based power cycle for working fluids

Figure 4 demonstrates the efficiency of energy and exergy for the fluids. As seen in the figure, the highest efficiency of energy, with 10.09 %, is when R41 is used. The lowest energy efficiency is 9.86% when R170 is used. Parallel to this, the highest exergy efficiency emerged when R41 was used, as in energy efficiency. The lowest exergy efficiency was calculated as 10.57% when using R170 fluid.

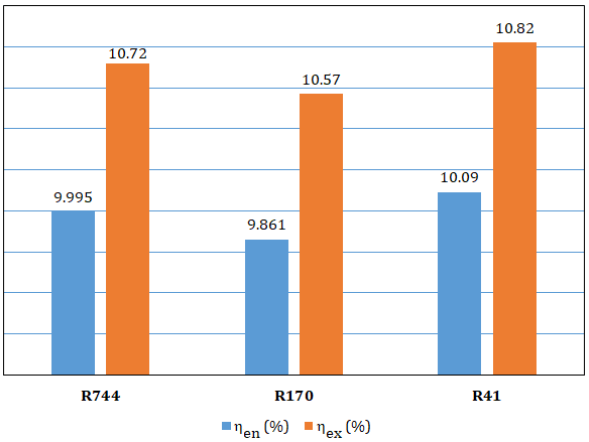

Figure 4. Efficiencies of energy and exergy from PV/T-based power cycle for working fluids

Figure 5 shows the PV/T surface temperature and the outlet temperature of the working fluid. As seen in the figure, the highest PV/T surface temperature was calculated when 56.48°C and R41 fluid were used. In addition, the exit temperature of the R41 fluid from the PV/T is the highest among the fluids at 52.35°C. It has been determined that the lowest PV/T surface temperature and the lowest outlet temperature of the fluid occur when R170 fluid is used.

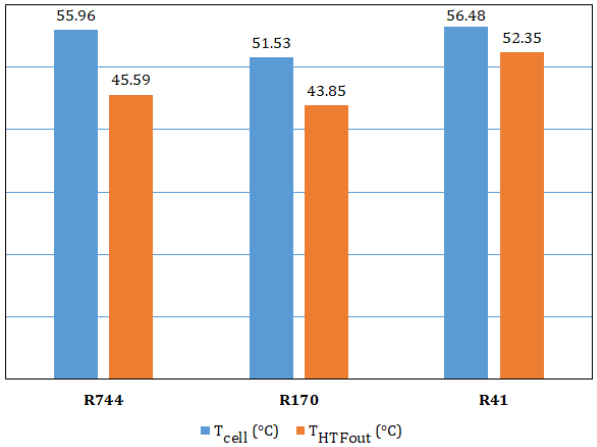

Figure 5. PV/T surface temperature and heat transfer fluid outlet temperature for working fluids

Figure 6 gives the result of exergy destruction. Contrary to the exergy efficiency analysis result, the maximum destruction of the exergy rate was determined for R170, succeeded by R744 and R41. The results show that 20.57 kW of exergy was destroyed using R170 for PV/T assisted power cycling, which corresponds to the minimum efficiency of exergy among selected fluids with a value of 10.57%.

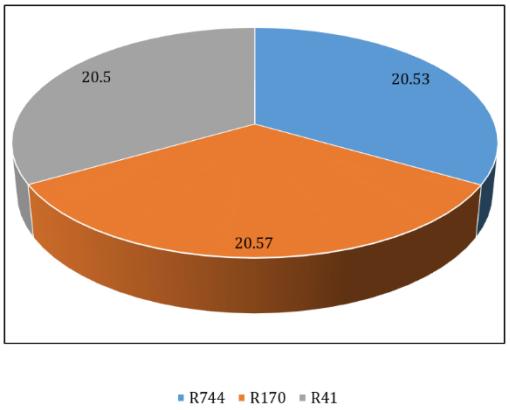

Figure 6. Exergy destruction of PV/T-based power cycle for working fluids

To determine the impact of P_1/P_2, that is the inlet pressure of the turbine, on PV/T driven system performance, a parametric analysis was conducted. All other variables remained constant while the pressure ratio was changed between 0.8 and 1.6. Figure 7 indicates the change in the net power obtained from the PV/T-based system with the pressure ratio. The chart shows that for whole fluids, the net power production rises with increasing P_2/P_1. But the rate of rise begins to somewhat slow down about 1.3, and beyond 1.6, there is no further increase in power generation. The fundamental cause of this is because as the pressure ratio rises, the pump's energy consumption does as well. Figure 8 shows how the efficiency of energy varies with P_1/P_2 for various working fluids. The net power generation and energy efficiency given in Figure 7 show almost the same trend.

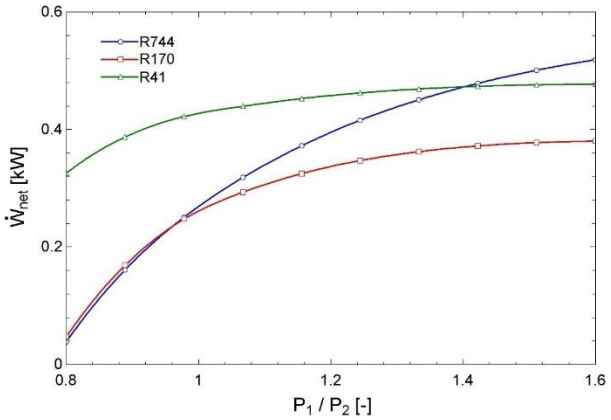

Figure 7. Change of the net power gained from the PV/T-based system with the P_1/P_2

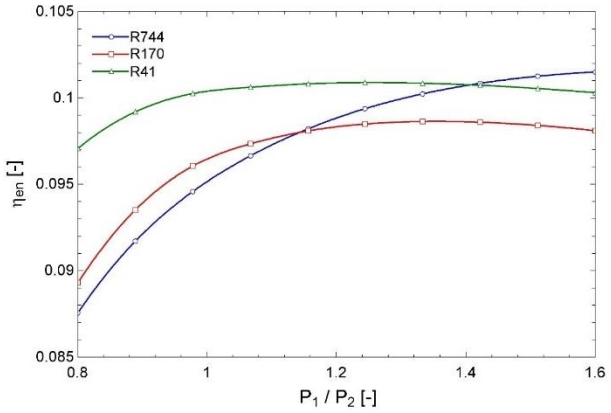

Figure 8. Change of the efficiency of energy obtained from the PV/T-based system with the pressure ratio

Figures 9 and 10 are displayed for the destruction rate of exergetic and efficiency of exergetic, respectively, for the effect of P_1/P_2 on the second law properties of the PV/T-based cycle. For all supercritical fluids, as the P_1/P_2 rises, exergy destruction decreases. But near 1.6 P_2/P_1, the exergy efficiency starts to follow an almost direct line, meaning there is no change in exergy destruction. On the other hand, the efficiency of exergy rises for whole working fluids. As with exergy destruction, the exergy efficiency starts to be constant near the 1.6 P_2/P_1. These results basically count on the thermophysical characteristics of the fluids.

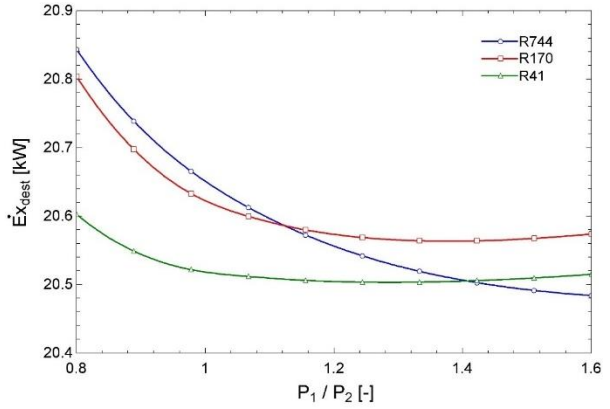

Figure 9. Change of the destruction of exergy obtained from the PV/T-based system with the pressure ratio

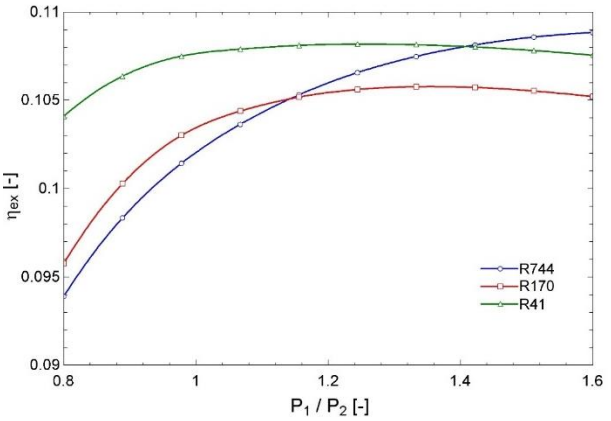

Figure 10. Change of the efficiency of exergy gained from the PV/T-based system with the pressure ratio

Another significant parameter affecting system performance is solar irradiation. For this purpose, parametric analyzes were conducted to examine the effect of solar irradiation on net power production, the efficiency of energy, destruction rate of exergy, and efficiency of exergy. Figure 11 illustrates the net power production versus solar radiation. As can be seen from the figure, the R170 has the lowest power production. Figure 12 demonstrates the efficiency of energy change with solar irradiation. Efficiency of energy for all working fluids increases with temperature. But after about 700 W/m^2 for R744, the slope of rise is almost constant after 1000 W/m^2 for R170 and R41.

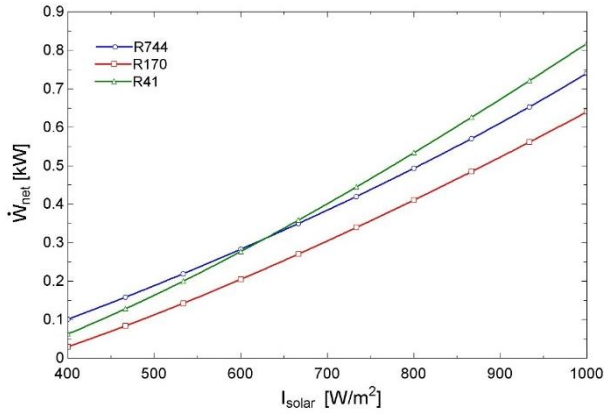

Figure 11. Change of the net power gained from the PV/T-based system with solar irradiation

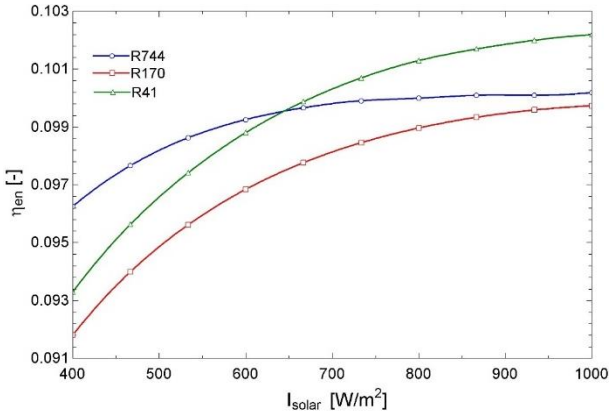

Figure 12. Change of the efficiency of energy obtained from the PV/T-based system with solar irradiation

The influence of solar irradiation on the destruction of exergy and the efficiency of exergy is given in Figures 13 and 14. As seen in Figure 13, exergy destruction is almost the same for all fluids, and exergy destruction increases as solar irradiation increases. Likewise, the exergy efficiency increases with solar irradiation, as seen in Figure 14. As in Figure 12, the exergy efficiency became constant after about 700 W/m^2 solar irradiation value for R744 and after about 1000 W/m^2 solar irradiation value for R170 and R41. The highest exergy efficiency belongs to R744, with approximately 10.35% at 400 W/m^2 solar irradiation. When solar irradiation rises to 1000 W/m^2, the highest exergy efficiency belongs to R41, with about 11%.

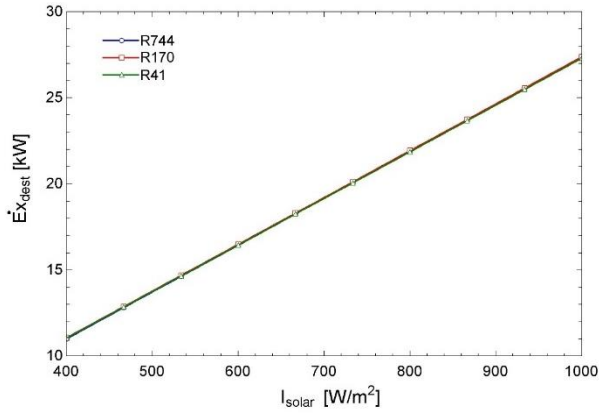

Figure 13. Change of the destruction of exergy obtained from the PV/T-based system with solar irradiation

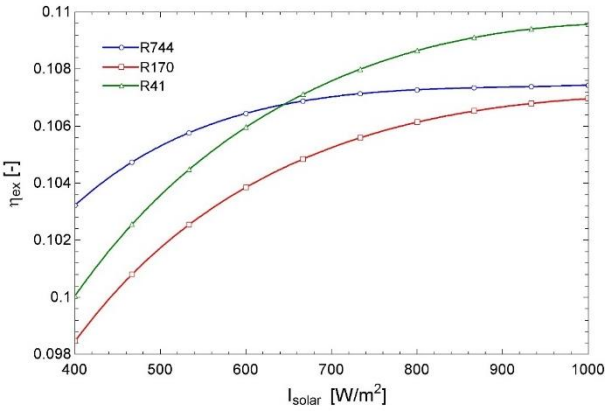

Figure 14. Change of the exergy efficiency obtained from the PV/T-based system with solar irradiation

6. Conclusions

In this research, a performance assessment of a PV/T-driven transcritical Rankine cycle was performed for various supercritical fluids. Analyzes were conducted for three different supercritical fluids, R744, R170, and R41. According to the results of the analysis, it was calculated that the highest power production rate was observed for the system using R41 with 0.4669 kW net power and 10.82% efficiency of energy. It was found that after R41, the best working one was R744, followed by R41 and R170. The fluids selected are both natural and non-toxic working fluids with zero ODP and relatively lower GWP. R41 has a critical temperature of about 44 °C, R744 and R170 about 30 °C. However, while R170 is flammable, R744 is not, so special attention should be paid to the use of R170. According to the analysis, the highest destruction rate of exergy occurred in the cycle using R170 with a value of 20.57 kW, followed by R744 and R41. These results indicate that among the fluids studied in this research, R41 and R744 have great potential for transcritical power production applications using lower-order thermal energy. Additionally, parametric analyzes were performed to determine the effects of P_1/P_2 and solar irradiation on the performance of the system, like power production, efficiency of energy, destruction of exergy, and efficiency of exergy. It has been shown that power generation rate, energy efficiency, and efficiency of exergy increase with P_1/P_2 and solar irradiation for all fluids. While the destruction of exergy decreases with increasing pressure ratio, exergy destruction increases with increasing solar irradiation. As a result, the use of supercritical working fluids in thermodynamic cycles has some advantages because of their low critical points. However, further research needs to be done to investigate the utilization of these fluids for different system parameters such as ambient temperature, cooling water temperature, environmental concerns, economic criteria, etc. The results of this research give short knowledge about the use of supercritical fluids in PV/T assisted transcritical power cycle. In future studies, it is aimed to examine the system performance by using new generation working fluids.

References

[1] Kizilkan Ö. Evaluation of Transcritical Rankine Cycle Driven by Low - Temperature Geothermal Source for Different Supercritical Working Fluids. *International Journal of Technological Sciences,* 3(11), 155-169, 2019.

[2] Soytürk Yıldırım G. *Faz Değiştiren Madde ile Güneş Enerjisinin Depolanmasının ve Isıtma Uygulamalarında Kullanımının İncelenmesi*. MSc Thesis, Süleyman Demirel University, Isparta, Turkey, 2018 (In Turkish).

[3] Kazemian A, Taheri A, Sardarabadi S, Ma T, Fard MP, Peng J. Energy, Exergy and Environmental Analysis of Glazed and Unglazed PVT System Integrated with Phase Change Material: An Experimental Approach. *Solar Energy,* 201, 178-189, 2020.

[4] Shiroudi A, Taklimi SRH, Mousavifar SA, Taghipour P. Stand-Alone PV-Hydrogen Energy System in Taleghan-Iran Using HOMER Software: Optimization and Technoeconomic Analysis. *Environmental Development and Sustainable,* 15, 1389–1402, 2013.

[5] Ma T, Yang H, Zhang Y, Lu L, Wang X. Using Phase Change Materials in Photovoltaic Systems for Thermal Regulation and Electrical Efficiency Improvement: A Review and Outlook. *Renewable and Sustainable Energy Reviews,* 43, 1273-1284, 2015.

[6] Babayan M, Mazraeh AE, Yari M, Niazi NA, Saha SC. Hydrogen Production with a Photovoltaic Thermal System Enhanced by Phase Change materials,

Shiraz, Iran case study. *Journal of Cleaner Production*, 215, 1262-1278, 2019.

[7] Gül M, Akyüz E. Hydrogen Generation from a Small-Scale Solar Photovoltaic Thermal (PV/T) Electrolyzer System: Numerical Model and Experimental Verification. *Energies,* 13, 2997, 2020.

[8] Sachit FA, Rosli MAM, Tamaldin N, Misha S, Abdullah AL. Nanofluids used in Photovoltaic Thermal (PV/T) Systems: A Review. *International Journal of Engineering & Technology,* 7, 599-611, 2018.

[9] Zulkepli A, Ibrahim H, Alias A, Azran Z, Basrawi F. Review on the Recent Developments of Photovoltaic Thermal (PV/T) and Proton Exchange Membrane Fuel Cell (PEMFC) Based Hybrid System. *MATEC Web of Conferences*, 74, 00019, 2016.

[10] Solimpeks. https://www.solimpeks.com.tr/ (Date of Access: 17.03.2023)

[11] Tchanche BF, Lambrinos G, Frangoudakis A, Papadakis G. Low-Grade Heat Conversion into Power Using Organic Rankine Cycles – A Review of Various Applications. *Renewable and Sustainable Energy Reviews,* 15, 3963-3979, 2011.

[12] He C, Liu C, Gao H, Xie H, Li Y, Wu S, Xu J. The Optimal Evaporation Temperature and Working Fluids for Subcritical Organic Rankine Cycle. *Energy,* 38, 136-143, 2012.

[13] Peris B, Navarro-Esbri J, Moles F, Collado R, Mota-Babiloni A. Performance Evaluation of an Organic Rankine Cycle for Power Applications from Low Grade Heat Sources. *Applied Thermal Engineering* 75, 763-769, 2015.

[14] Sun J, Liu Q, Duan Y. Effects of Evaporator Pinch Point Temperature Difference on Thermo Economic Performance of Geothermal Organic Rankine Cycle Systems. *Geothermics,* 75, 249 - 258, 2018.

[15] Wang X, Levy EK, Pan C, Romero CE, Banerjee A, Maya CB, Pan L. Working Fluid Selection for Organic Rankine Cycle Power Generation Using Hot Produced Supercritical CO_2 from a Geothermal Reservoir. *Applied Thermal Engineering, 149*, 1287–1304, 2019.

[16] Bahrami M, Pourfayaz F, Kasaeian A. Low Global Warming Potential (GWP) Working Fluids (WFs) for Organic Rankine Cycle (ORC) Applications. *Energy Reports*, 8, 2976-2988, 2022.

[17] Thurairajaab K, Wijewardane A, Jayasekara S, Ranasinghe C. Working Fluid Selection and Performance Evaluation of ORC. *Energy Procedia,* 156, 244-248, 2019.

[18] Ganjehsarabi H. Mixed Refrigerant as Working Fluid in Organic Rankine Cycle for Hydrogen Production Driven by Geothermal Energy. *International Journal of Hydrogen Energy*, 44, 18703-18711, 2019

[19] Yu H, Kim D, Gundersen T. A Study of Working Fluids for Organic Rankine Cycles (ORCs) Operating Across and Below Ambient Temperature to Utilize Liquefied Natural Gas (LNG) Cold Energy. *Energy,* 167, 730-739, 2019.

[20] Song C, Gu M, Miao Z, Liu C, Xu J. Effect of Fluid Dryness and Critical Temperature on Transcritical Organic Rankine Cycle. *Energy,* 174, 97-109, 2019.

[21] Xu W, Deng D, Zhang Y, Zhao D, Zhao L. How to Give a Full Play to the Advantages of Zeotropic Working Fluids in Organic Rankine Cycle (ORC). *Energy Procedia,* 158, 1591-1597, 2019.

[22] Wang E, Zhang M, Meng F, Zhang H. Zeotropic Working Fluid Selection for an Organic Rankine Cycle Bottoming with a Marine Engine. *Energy,* 243, 123097, 2022.

[23] Han J, Wang X, Xu J, Yi N, Talesh SSA. Thermodynamic Analysis and Optimization of an Innovative Geothermal-Based Organic Rankine Cycle Using Zeotropic Mixtures for Power and Hydrogen Production. *International Journal of Hydrogen Energy*, 45, 8282-8299, 2020.

[24] Karellas S, Schuster A. Supercritical Fluid Parameters in Organic Rankine Cycle Applications. *International Journal of Thermodynamics,* 11(3), 101-108, 2008.

[25] Radulovic J. Utilisation of Fluids with Low Global Warming Potential in Supercritical Organic Rankine Cycle. *Journal of Thermal Engineering,* 1(1), 24-30, 2015.

[26] Bolaji BO, Huan Z. Ozone Depletion and Global Warming: Case for the Use of Natural Refrigerant. *Renewable and Sustainable Energy Rewiews* 18, 49-54, 2013.

[27] Refrigerants naturally, C/O Heat International, http://www.refrigerantsnaturally.com/ (Date of Access: 16.03.2023)

[28] Sakellariou E, Axaopoulos P. An Experimentally Validated, Transient Model for Sheet and Tube PVT Collector. *Solar Energy,* 174, 709-718, 2018.

[29] Sarhaddi F, Farahat S, Ajam H, Behzadmehr A, Adeli MM. An Improved Thermal and Electrical Model for a Solar Photovoltaic Thermal (PV/T) Air Collector. *Applied Energy,* 87, 2328-2339, 2010.

[30] Cengel YA, Boles MA. *Thermodynamics: An Engineering Approach 8th Edition*, 2015.

[31] Bejan A, Moran MJ. *Thermal Design and Optimization*, New York: John Wiley & Sons,1996.

[32] Dincer I, Rosen MA. *Exergy: Energy, Environment and Sustainable Development*, 2013.

[33] Kalogirou S. *Solar Energy Engineering Processes and System.* Elsevier, 2009

[34] Çengel YA. *Heat and Mass Transfer.* İzmir Güven Bookstore, Güven Scientific, 2011 (in Turkish)

[35] Yazdanifard F, Ebrahimnia-Bajestan E, Ameri Mehran. Investigating the Performance of a Water-Based Photovoltaic/Thermal (PV/T) Collector in Laminar and Turbulent Flow Regime. *Renewable Energy,* 99, 295-306, 2016.

[36] Soteris A, Sotirios K, Konstantinos B, Camelia S, Viorel B. Exergy Analysis of Solar Thermal Collectors and Processes. *Progress in Energy and Combustion Science*, 56, 106–137,2016.